Acc. Chem. Res. **2001,** *34,* 607−614

Why Is It So Difficult To Simulate Entropies, Free Energies, and Their Differences?

WILLIAM P. REINHARDT,*
MARK A. MILLER, AND LYNN M. AMON
Department of Chemistry, Box 351700, University of Washington, Seattle, Washington 98195-1700

Received November 29, 2000

ABSTRACT

The classical 19th century thermodynamic inequalities of Clausius and Helmholtz are applied to the calculation of entropy and free energy changes by computer simulation. The irreversibility of finite-time thermodynamic paths is exploited to obtain upper and lower bounds on these quantities. Schrödinger's microscopic interpretation of heat and work provides the basis for a literal implementation of the key historical concepts on the computer using the Monte Carlo algorithm of Metropolis. Coupling schemes, paths, and reference states are variationally optimized to improve the convergence of the simulated properties, and a newly introduced variational flexibility, metric scaling, is overviewed. Reasons for expecting limiting power laws for the convergence are outlined.

I. Introduction: The Second Law

"Free energy is arguably the most important general concept in physical chemistry", wrote Peter Kollman in an overview[1] of the difficulties and progress in the computational thermodynamics of hard-core fluids. Chemists are well aware that entropies and free energies determine equilibrium constants and the direction of spontaneous chemical change. Indeed, one might think that intellectual development of these basic concepts ended in the 19th century. It is therefore interesting to note that biochemists now work with standard free energies constrained to the in vivo conditions of constant temperature, pressure, and pH,[2] rather than the traditional but less appropriate constraints of constant temperature and pressure, or temperature and volume. Thermodynamics is now applied to individual macromolecules in solution, and the protein folding problem has been formulated in terms of free energy landscapes, upon which the native state is thought to reside at the bottom of a funnel.[3] These developments could hardly have been foreseen by the founding figures of thermodynamics. Furthermore, despite being a property of equilibrium systems, free energy also plays an important role in kinetics, since the rate of a reaction may be controlled by free energy barriers and entropic bottlenecks.[4]

The utility of free energy in determining the directionality of a chemical process has its historical basis in the Second Law of thermodynamics as elucidated by Carnot and Clausius: spontaneous processes are those for which the entropy of the universe, consisting of the system and its surroundings, increases. Helmholtz and Gibbs recast this result in terms of the properties of the system itself under external thermodynamic constraints. In this Account, we explore the direct translation of the Clausius and Helmholtz results, involving heat and external work respectively, into a computational algorithm for obtaining entropy and free energy changes. To do so, we need an interpretation of heat, work, and thermodynamic constraints both at a molecular level and in the context of computer simulation. The microscopic approach contrasts sharply with that of traditional phenomenological thermodynamics, whose development is independent of any particulate theory of matter.[5]

Since entropy and free energy are state functions, there exists great freedom in the choice of thermodynamic path for calculating changes in these properties; the result must be independent of the path. If the path is traversed reversibly, then the entropy and free energy changes can be expressed in terms of the heat and work expended. However, if we are literally to mimic thermodynamic processes by computer simulation, the paths must be traversed in a finite time, hence irreversibly. Under irreversible conditions, the important expressions are the thermodynamic inequalities rather than the equalities. In other words, by calculating the irreversible heat and work, one obtains bounds to entropy and free energy changes rather than the changes themselves. The choice of path is then no longer moot, since it determines the extent of irreversibility and consequently the tightness of the bounds. Thus, there is a variational principle: the path may be optimized to produce the closest upper and lower bounds in a specified (computer) time.

Although methods for computing free energy changes have existed for decades, actual computations are still time-consuming. The longest-established techniques are thermodynamic integration[6] and free energy perturbation.[7] Both use equilibrium simulations and invoke reversible paths. Even so, the choice of path matters because finite simulations carry statistical errors, and the path determines the size of these errors. In this Account, we focus on an alternative approach, developed over the past decade in our research group. (Other methods have been reviewed elsewhere.[8]) Our finite-time variational method is manifestly nonequilibrium and provides a systematic basis for the optimization of paths to obtain rapidly converging bounds on entropy and free energy changes. The introduction of irreversibility puts our method into

William Reinhardt has received degrees from U.C. Berkeley (B.S. in basic chemistry), Harvard (A.M. in chemistry, Ph.D. in chemical physics), and the University of Pennsylvania (M.A., hon.). In addition to computational thermodynamics, he is currently studying coherent matter waves and many-body theory in Bose−Einstein condensates.

Mark Miller holds an M.A. in natural sciences and a Ph.D. in theoretical chemistry (supervised by Dr. David Wales) from Cambridge University. He currently works on computational thermodynamics as a postdoctoral fellow in Chemistry at the University of Washington.

Lynn Amon earned her B.S. in chemistry at Saint Mary's College, Notre Dame, and her Ph.D. from the Chemistry Department at the University of Washington. She is now a postdoctoral fellow in Bioengineering at the University of Washington.

10.1021/ar950181n CCC: $20.00
Published on Web 05/10/2001

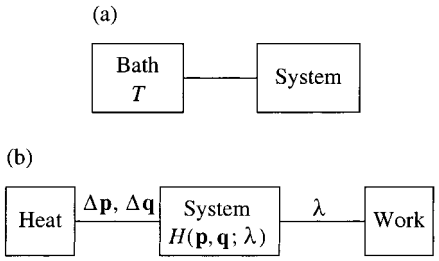

FIGURE 1. (a) Traditional thermodynamic idealization of an isolated system coupled to a heat bath. (b) Scheme for finite-time variational calculations of free energy changes. The parametrized Hamiltonian, $H(\lambda)$, defines the system. The particle positions, **q**, and momenta, **p**, are coupled to the heat bath, and the switching parameter, λ, couples the system to a source of external work.

the realm of finite-time thermodynamics.[9] A connection between the key results of that field and our variational switching calculations has been provided by Schön.[10]

The Account proceeds as follows. In section II, the finite-time variational method is described and applied to the entropy change of a model system by monitoring heat flow and invoking Clausius's inequality (a statement of the Second Law). In section III, the method is extended to free energy changes using Helmholtz's inequality and a microscopic interpretation of work. Section IV addresses the variational optimization of paths and reference states. In section V, the distance metric in configuration space is exploited as an additional variational flexibility. In section VI, the limiting power laws for the convergence of entropy and free energy bounds are discussed. Section VII provides a brief summary.

II. Heat: Clausius Meets Metropolis

Thermodynamics relies on an idealization of reality and yet yields quantitatively correct predictions for real systems at equilibrium. Perhaps the primary idealization is the conceptual separation of an equilibrium system from its environment. The environment is replaced by simply stated macroscopic external constraints such as temperature, pressure, pH, etc., implying that, at equilibrium, the system attains the same values of these control parameters. Figure 1a exemplifies such an idealization. The system is in contact with a thermal reservoir that has a well-defined and controllable temperature, T. The reservoir is a thermostat for the system, and T is a property of the thermostat. In what follows, we will never need to know the temperature of the system; we merely note that at equilibrium it is identical to T.

The state of a system may be changed by bringing it into contact with different environments, which admit the possibilities of heat flow and external work. In the 1850s, Clausius analyzed the reversible heat, Q^{rev}, transferred while taking a system through a cycle of changes that eventually return it to its original state,[11] thereby identifying entropy (the integral of $\mathrm{d}Q^{\mathrm{rev}}/T$) as a state function. For processes where the heat flows irreversibly, an early statement of the Second Law yielded what we now call Clausius's inequality:

$$\int \delta Q/T \le \Delta S \tag{1}$$

with equality only in the limit $\delta Q = \mathrm{d}Q^{\mathrm{rev}}$. We emphasize that T in this inequality is the temperature of the heat bath; if heat flows irreversibly, the system itself is out of equilibrium and does not even possess a well-defined temperature.

Rather than regarding the inequality of expression (1) as a defect, we note that if the integration between the two thermodynamic states is carried out in both directions, upper and lower bounds to ΔS may be obtained from finite-time (and therefore irreversible) processes. Thus, a quantitative assessment of the systematic error due to irreversibility is available in addition to the ever-present statistical errors.

To use Clausius's inequality in a computer simulation, we need to establish the analogue of the thermostat with infinite thermal mass, full temperature control, and mechanism for heat transfer with the system. Although not usually regarded from this literal point of view, the implicit thermostat in Metropolis Monte Carlo (MC) simulations[12] fulfills these requirements. The Metropolis algorithm (to be exemplified shortly) generates a chain of configurations, the probability of a given structure with potential energy V being proportional to its Boltzmann weight, ρ:

$$\rho = \exp(-V/kT) \tag{2}$$

This is the weight with which structures occur in the canonical ensemble (conditions of constant temperature, volume, and number of particles). Hence, the canonical value of a macroscopic observable can be found by averaging its instantaneous value over the chain of configurations. For example, the internal energy is the average of the total energy at constant temperature. Absolute entropies and free energies are harder to calculate because they cannot be expressed as such averages. The following example illustrates how the flow of heat between the system and thermostat in an MC simulation is interpreted and used to evaluate the integral in Clausius's inequality (1) directly.

Consider a system of N distinguishable uncoupled quantum harmonic oscillators, each with a quantum number $v = 0, 1, 2, \ldots$ and corresponding energy levels $E_v = (v + 1/2)\hbar\omega$. Specification of all N quantum numbers constitutes a configuration of this system. The oscillators are initially equilibrated at temperature T_1 using the following implementation of the Metropolis algorithm:

(a) An oscillator is chosen randomly.

(b) With equal probability, the quantum number of the oscillator is either raised or lowered by 1.

(c) If the energy is lowered, the change is accepted unless the quantum number has become negative, in which case the change is rejected.

(d) If the energy is raised, the Boltzmann factor $\rho = \exp(-\hbar\omega/kT_1)$ is computed, and the change is accepted with probability ρ by comparing a random number between 0 and 1 with ρ.

(e) If a move is rejected, the previous configuration is recounted.

(f) Steps (a)−(e) are repeated until the populations of the quantum states stop evolving, i.e., equilibrium is attained. Each cycle through these steps adds a configuration to the chain being generated.

Now let us calculate the entropy change for a simple process in which the temperature increases to T_2. This is accomplished by continuing the simulation as prescribed above, but incrementing the temperature after each step. We perform this gradual switching over M simulation steps, adding $(T_2 - T_1)/M$ to the temperature at each step.

As the temperature rises, there must be a net flow of heat into the system. At this point we take the Metropolis thermostat literally: if an MC move is accepted, the energy of the system changes, and the only source of this energy is the notional heat bath. Hence, the change in energy of the system can be identified with the flow of heat from the bath to the system. If a move is rejected, there is no heat flow. For each element of heat, δQ, the temperature of the heat bath is known, and the integrand in Clausius's inequality (1) can be evaluated. Note that when the temperature stops changing, the system is out of equilibrium. Heat will continue to flow until equilibration at temperature T_2 is achieved, and it is important to continue the simulation and collect the remaining heat at constant temperature after T_2 has been reached.

This procedure directly furnishes a lower bound to ΔS for the temperature change. By equilibrating at T_2 and then gradually lowering the temperature to T_1, again accumulating $\delta Q/T$ until equilibrium is regained at the end, one obtains a lower bound to the entropy change for the reverse process, $-\Delta S$, i.e., an upper bound to ΔS itself. Hence, switching in both directions between two thermodynamic states yields both lower and upper bounds to the entropy change.

The solid lines in Figure 2 show the upper and lower bounds to the entropy change of a system of quantum harmonic oscillators whose temperature is doubled. Successive points were derived from simulations with an increasing number, M, of switching steps plus a fixed number of additional steps for final re-equilibration. For small M, the change to the temperature at each MC step is relatively large and the system falls far from equilibrium, resulting in a wide separation of the bounds. For larger M, the temperature increments are smaller and the process is more reversible, resulting in tighter bounds. The bounds gradually converge to the correct value, which is analytically known for this simple system.

What can be done to make the bounds converge more rapidly? Although the Metropolis algorithm is not concerned with the physical nature of the thermostat, it does require a mechanism for the coupling of the thermostat to the system. The coupling is manifest in the MC move set; in the above example, trial moves consisted of changing the quantum number of a randomly chosen oscillator by ±1. The dashed lines in Figure 2 show how the convergence of the bounds is improved by allowing changes in the quantum number of up to $\pm kT_1/\hbar\omega$. This modification corresponds to a stronger coupling with the heat bath and the ability to explore state space more rapidly, enabling faster equilibration of the system.

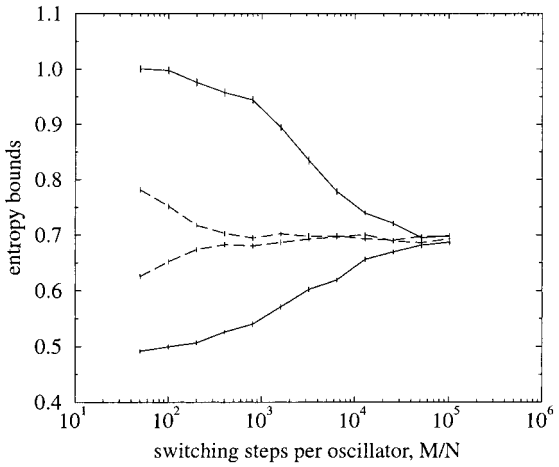

FIGURE 2. Bounds to the entropy change of 4000 quantum harmonic oscillators ($\hbar\omega = 1$) for a linear temperature change from $kT = 10$ to $kT = 20$. The horizontal axis shows the number of MC moves over which the temperature was changed. An additional 10 000 moves per particle were performed at the end of each simulation to accumulate the remaining heat required for equilibration. (Solid) Weak coupling to the heat bath ($\delta n = \pm 1$ allowed); (dashed) strong coupling ($\delta n = \pm 1, \pm 2, ..., \pm 20$). The bars indicate the standard error over 25 runs.

From this simple numerical experiment, we conclude that the Metropolis thermostat may be treated like a real thermostat, and that by keeping track of heat flowing in and out of the bath, one may calculate bounds to entropy changes by direct application of Clausius's fundamental inequality. Since the Helmholtz free energy is defined by $A = U - TS$, where U is the internal energy (in principle, a straightforward ensemble average), the ability to calculate ΔS as above could be seen as a route to obtaining free energy changes. However, this turns out to be highly inefficient. In addition to the potentially time-consuming necessity of accumulating heat after the final conditions have been reached, and of calculating ΔU separately, the bounds to ΔS never converge more rapidly than a constant divided by $M^{1/2}$ (see section VI). The next section shows that we can do better by considering external work.

III. Work: Enter Helmholtz and Schrödinger

Often, rather than simply changing the temperature, as in the example of section II, one wants to change the interactions between the particles that constitute the system itself. For example, knowing the free energy difference between a liquid and the ideal gas, where the molecules do not interact at all, puts the free energy of the liquid on an absolute scale, since the absolute free energy of the ideal gas is analytically known. In a solution, modification of the solvent−ion interaction potential permits direct comparison of the solvation free energies of different ions.

Such processes may be formulated by devising a parametrized Hamiltonian, $H(\lambda)$, which switches smoothly between the system of interest at $\lambda = 0$ and the reference state at $\lambda = 1$. The traditional techniques[8] of thermody-

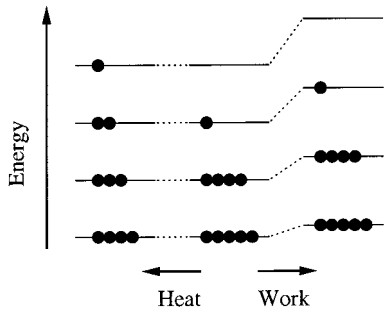

FIGURE 3. Schematic energy levels and populations in Schrödinger's interpretation of heat and work in statistical mechanics. Starting at the center, heat supplied to the system promotes molecules to higher states, whereas work done on the system raises the energies of the levels at constant population.

namic integration and free energy perturbation express the free energy difference between the two states in terms of equilibrium ensemble averages at a series of intermediate values of the switching variable, λ. In the limit where a single configuration is taken to represent each average, but the number of intermediate points between $\lambda = 0$ and 1 is very large, both techniques reduce to the slow growth method.[13] At this extreme, the system lags behind the changing Hamiltonian, producing hysteresis when the direction of change is reversed.

A fresh physical perspective was introduced in 1992 by Reinhardt and co-workers[14,15] in an analysis summarized by Figure 1b. Here, the system is coupled not only to a thermostat, but also to a source of external work. Both heat transfer and external work alter the energy of the system, and the distinction between these two processes in statistical mechanics is provided by Schrödinger's interpretation.[16] In the example of section II, the flow of heat caused the quantum numbers of the oscillators to change, thereby altering the populations of the quantum states. In that example, the Hamiltonian was fixed, and the energies of the states remained constant as the temperature was changed. If the Hamiltonian changes, the populations of the states remain instantaneously fixed, but the energies of the states change. It is the corresponding change in the system's energy that Schrödinger classified as work. This interpretation is shown schematically in Figure 3 and is summarized by the equation

$$\delta W = \sum_{\nu} n_{\nu}\, \delta E_{\nu} + \sum_{\nu} E_{\nu}\, \delta n_{\nu} \qquad (3)$$

where n_ν and E_ν are the population and energy of level ν, respectively. The first sum in eq 3 is the work, and the second is the heat.

By changing the Hamiltonian gradually from $H(\lambda = 0)$ to $H(\lambda = 1)$ over the course of an MC simulation, one can accumulate the external work, W, required to take the system between the two states in analogy with section II, where the temperature was slowly switched and the heat was accumulated. Since the Hamiltonian must be changed at a finite rate, the work is irreversible, and under conditions of constant volume, temperature, and number of particles, it is an upper bound to the free energy change,

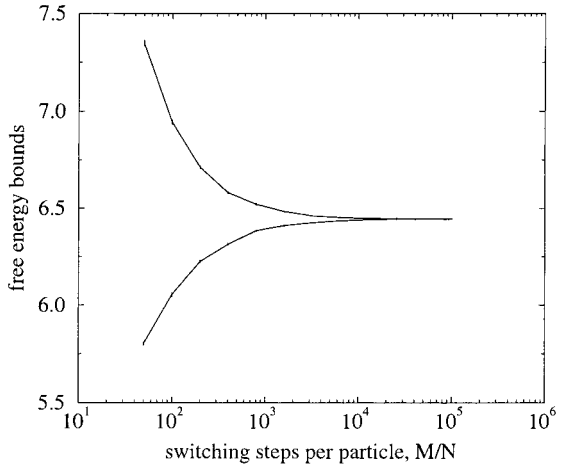

FIGURE 4. Bounds to the free energy change of 4000 quantum harmonic oscillators at $kT = 10$ for a change in oscillator frequency from $\hbar\omega = 1$ to $\hbar\omega = 2$.

according to Helmholtz's inequality:[17]

$$W \geq \Delta A \qquad (4)$$

where A is the Helmholtz free energy, and the equality applies only in the reversible limit. A lower bound to ΔA may be obtained by switching in the reverse direction, from $H(\lambda = 1)$ to $H(\lambda = 0)$.

Figure 4 shows upper and lower bounds to the free energy change of the quantum harmonic oscillator system. In this example, the temperature is held fixed, but the frequency, $\hbar\omega$, of the oscillators is doubled over the course of the simulation. As soon as the Hamiltonian stops changing, no further work is done. Therefore, there is no need to continue the simulation until equilibrium has been reached at the final state.

Another way to obtain the work is to invoke the First Law: $\Delta U = W + Q$. ΔU is simply the energy difference between the initial and final configurations in the simulation, and Q can be obtained as in section II. When the Hamiltonian has stopped changing, any further changes in Q exactly match changes in ΔU, leaving W unchanged. This identity will be useful in the next section, where classical interacting systems are considered. In classical statistical mechanics, the analogue of a quantum state is the configuration, so that heat is the energy required to change the configuration, whereas work is the energy change at fixed configuration due to a change in the classical Hamiltonian. For such systems, it is usually more convenient to accumulate the heat transferred in each MC step than to compute the work, since δQ must already be calculated to evaluate the acceptance probability at each step.

The parametrization of the Hamiltonian presents a variational freedom in addition to the coupling with the thermostat described in section II. A well-chosen path between the two thermodynamic states of interest will minimize the irreversibility of the work, resulting in tighter bounds on the free energy. For the simple oscillator system described here, a simple linear change of $\hbar\omega$ with the switching variable, λ, is effectively optimal, but for

interacting systems the choice is more complex. The next section addresses these issues.

IV. Optimization of Paths and Reference States

We now apply finite-time variational switching to a classical 55-atom argon cluster,[19] Ar_{55}, modeling the interatomic Hamiltonian by the Lennard-Jones potential,[18] V_{LJ}. We focus on determining the absolute free energy of this cluster by calculating the free energy difference from a non-interacting reference state of known free energy. This is achieved by gradually reducing the strength of particle interactions to zero during the simulation. We will see that the rate of convergence of the bounds on ΔA is affected by the choices of reference state[19] and switching path.

An obvious choice of reference state here is a system of 55 non-interacting atoms, i.e., an ideal gas confined to a specified volume. The volume constraint is easily achieved in an MC simulation by rejecting any moves that take an atom outside the container. This same container must also be applied to the interacting cluster, resulting in a volume-dependent free energy as the atoms move around the box. We eliminate overall translation by defining the container relative to the location of the cluster. If a single atom is used to define the location, the free energy of the ideal gas reference state under the same volume constraint can be calculated analytically.[19] However, the box must then be at least twice the size of the cluster to accommodate all possible cluster rotations. A large box is not optimal because the phase space that must be explored becomes enormous, impairing the simulation. If the location of the cluster is instead defined by the cluster's center-of-mass, then a box only slightly larger than cluster itself is required to accommodate overall rotation. The center-of-mass constraint requires a slightly more sophisticated MC algorithm that consumes more time per simulation step. Furthermore, the free energy of the ideal gas reference state with this constraint is not so straightforward. However, there exists an exact solution containing a one-dimensional integral that must be evaluated numerically.[20] Because the box is much smaller in the center-of-mass constrained calculation, we expect faster convergence of the bounds to ΔA. In Figure 5, we see precisely this behavior for a calculation at $T = 45$K. In (a) the simulation box is centered on the center-of-mass, and in (b) it is centered on one atom. The values of ΔA for the two calculations are different because the reference states are different, but the resulting absolute free energies are the same. The data are averages over 20 runs with different initial configurations, and the error bars represent the associated statistical uncertainty. Only such ensemble averages constitute bounds to ΔA; individual runs fluctuate about the mean.[15]

When the temperature is low and the cluster is solid-like,[21] the phase space can be trimmed even further. Since atoms do not exchange, instead of constraining all the atoms to one large box, each atom can be constrained to its own small box. Furthermore, the boxes can be defined not only with respect to the translational motion of the cluster but also with respect to its rotation. In this case, defining the location of the cluster at the center-of-mass results in a reference state with an unknown free energy that must be estimated numerically. Using a single atom to define the location, however, does produce a reference state with an analytically known free energy.[19] Because the whole cluster is not enclosed in this case, the volume penalty taken for this latter strategy is quite small, and the convergence of the bounds on ΔA (Figure 6) is actually better due to algorithmic complications with the center-of-mass constraint.

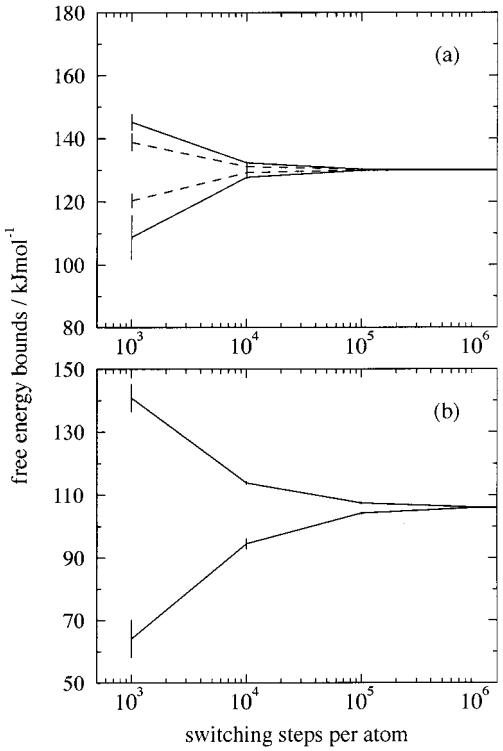

FIGURE 5. Upper and lower bounds[19] to ΔA for $Ar_{55} \rightarrow$ ideal gas at $T = 45$ K. (Solid) Switching path is $V(\lambda) = c(\lambda)V_{LJ}$ with $c(\lambda) = (1 - \lambda)^3$; (dashed) path with core-softening.[23] (a) Container centered at the center of mass; (b) container centered on one atom. The vertical ranges in (a) and (b) are the same for comparison of the convergence rates.

Another way to improve the convergence of the bounds is to optimize the switching path. We return to Ar_{55} at $T = 45$ K in a single container, defined with respect to the center-of-mass. A simple switching path between the initial Hamiltonian, $H(\lambda = 0) = V_{LJ}$, and the reference Hamiltonian, $H(\lambda = 1) = 0$, can be made by prefixing V_{LJ} with a coefficient, $c(\lambda)$, which changes continuously from unity at $\lambda = 0$ to zero at $\lambda = 1$. In contrast to thermodynamic integration, which employs the derivative $\partial H/\partial\lambda$, there are fewer restrictions[22] on the choice of $c(\lambda)$. However, the obvious choice of a linear relationship proves troublesome for small M (rapid switchings) because the atoms overlap in the ideal gas reference state, contributing arbitrarily strong repulsive interactions when the potential is turned on. When $c(\lambda) = (1 - \lambda)^3$, this problem is mostly overcome, as shown by the solid line in Figure 5a. The dashed line in Figure 5a represents calculations where $c(\lambda)$ was decreased linearly but V_{LJ} itself was also

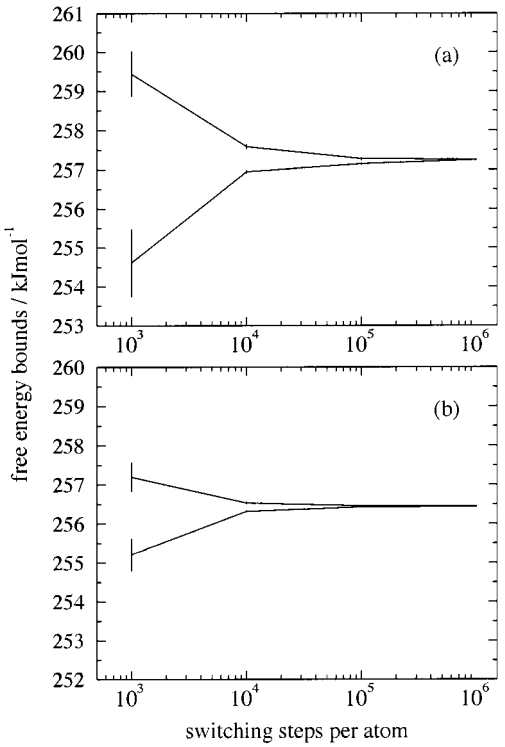

FIGURE 6. Upper and lower bounds[19] to ΔA for $Ar_{55} \rightarrow$ ideal gas at $T = 10$ K with individual boxes for each atom. (a) Boxes defined with respect to the center of mass; (b) boxes defined with respect to one atom.

modified during the switching so as to mitigate the repulsive core problem.[22] This more complicated function[23] improves the convergence.

De Koning et al. have pointed out an advantage of choosing paths where the Hamiltonian is simply prefixed by a switching coefficient.[24] Moving along such paths is equivalent to changing the temperature, since only the ratio of the Hamiltonian to the thermal energy appears in the Boltzmann factor. Therefore, all points along the path are physically meaningful, yielding the free energy as a continuous function of temperature from a single simulation.

V. Metric Scaling:[25] An Additional Path Flexibility

The work done in a variational switching calculation is irreversible because the changing Hamiltonian continually redefines the equilibrium distribution of configurations. Switching at finite speed forces the system to lag behind the instantaneous equilibrium. A good path minimizes departure from equilibrium when traversed at reasonable rates.

In some applications, general information is available about the two thermodynamic states to be connected. For example, if the shape of the system's container changes, particles must move out of areas that are to be eliminated and into new vacant ones. Such reorganizations often constitute the bottleneck in switching calculations; highly nonequilibrium configurations are generated if the particles jam together, and relaxation can be slow. Knowledge of the overall transformation to be effected can assist in guiding the system through the change.

Consider the Ar_{55} cluster of section V confined to a fairly tight spherical container at low temperature. To calculate the free energy change when this microcrystal is compressed, we might run a switching simulation in which the container wall interacts repulsively with the atoms and its radius is gradually decreased. Overall, the atoms would be forced inward, while undergoing the usual thermal fluctuations.

We can easily measure the average radial position of an atom at any point during the switching by performing a short simulation. Then, rather than leaving the atoms to find their way during a switching simulation, we can gradually scale their coordinates to bring them, on average, to the correct positions. This process can be regarded as a scaling of the distance metric in configuration space.[25] If viewed in the unscaled coordinates, the cluster would simply appear to undergo equilibrium fluctuations with no systematic evolution; by guiding the atoms to their natural positions in the switching, gross departure from equilibrium is avoided. Metric scaling effects a volume change, and an ideal-gas work-like correction of $kT \ln S$ must be subtracted from the free energy for each atom subjected to the scaling, where S is the ratio of the final scaled volume to the original volume available to the atom.[25]

Scaled coordinates have been used for some time in constant-pressure simulations, where the simulation cell dimensions fluctuate.[26] Such scaling is necessary to prevent periodic gaps or overlaps between cell images when periodic boundary conditions are used. In contrast, when metric scaling is applied to finite systems, the scaling schedule may be optimized independently of the container changes and may even differ from atom to atom, as illustrated in the following example.

At its global potential energy minimum, the Ar_{55} cluster has four geometrically distinct groups of atoms: 12 vertices, 30 edge atoms, a 12-atom icosahedral inner shell, and the central atom.[27] Each group responds differently when the cluster is compressed at low temperature. Figure 7 shows how metric scaling can improve the convergence of the free energy bounds. The long-dashed lines show the convergence for a volume change with no metric scaling. We then determined the average radial coordinate as a function of container radius during a rapid compression. The evolving average was fitted to a cubic polynomial in the switching parameter, λ. This function was then used to scale all the coordinates uniformly during a longer production run. The considerably tighter short-dashed bounds were obtained. Fitting a cubic to each of the four geometrically distinct groups of atoms separately and scaling the metric nonuniformly according to group yields some further improvement,[25] as shown by the solid lines.

Metric scaling has been successfully applied to cluster volume changes at higher temperatures and larger volumes. It has also been used to compare the free energy of body-centered cubic and face-centered cubic crystals directly.[25] These structures can be interconverted smoothly

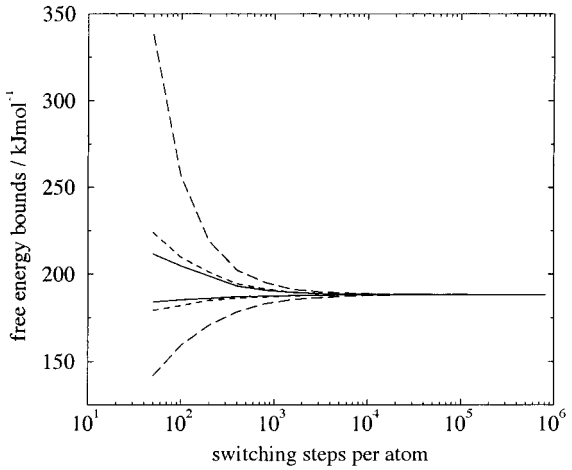

FIGURE 7. Bounds to the free energy change[25] of Ar_{55} for a container radius change between 0.817 and 0.612 nm at $kT = 24$ K. (Long dashes) No metric scaling; (short dashes) uniform metric scaling; (solid) nonuniform metric scaling. Corrections due to the intrinsic work of scaling are included.

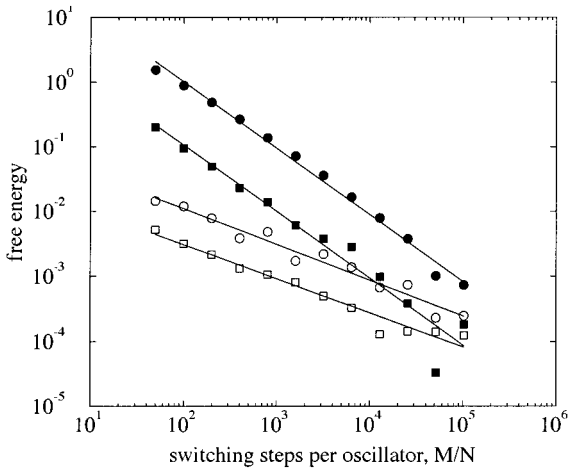

FIGURE 8. Convergence laws for the free energy of quantum harmonic oscillators when the energy level spacing changes from $\hbar\omega = 1$ to $\hbar\omega = 2$. (Solid symbols) Bound separation; (open symbols) uncertainty (standard error) in upper bound; (circles) conventional MC moves; (squares) moves chosen from the exact distribution. The lines are fits of $y = Cx^{-\alpha}$.

by a Bain distortion,[28] which is easily formulated as an anisotropic metric scaling.

One caution is advisable: metric scaling schedules must be determined only by the average response of a system to the changing Hamiltonian, and not by the trajectory under scaling itself. Use of specific or on-the-fly information introduces a Maxwell's daemon and systematic error.[15]

VI. How Quickly Can ΔS and ΔA Be Calculated?

If the computer time invested in a free energy calculation is doubled, how much improvement in precision can be expected? The foregoing sections showed that tighter bounds can be obtained by imaginative choice of coupling schemes, switching paths, and reference states. We now turn to the rate of convergence with M, the number of simulation steps.

Recall the quantum harmonic oscillator calculations of section III. We saw that the free energy bounds converge most rapidly when the state of the system is kept as close as possible to the instantaneous equilibrium at all points during switching. For harmonic oscillators, we know the distribution over states for any T and $\hbar\omega$ analytically. Therefore, instead of using a trial change in quantum number as the MC step, we could simply replace the existing quantum number of the randomly chosen oscillator with a new value chosen from the exact distribution. We expect this process to reduce the lag of the system to an absolute minimum and give us the best possible convergence of bounds.

Figure 8 shows the separation of the free energy bounds as a function of M for a change in oscillator strength from $\hbar\omega = 1$ to $\hbar\omega = 2$. Also shown is the standard error in the upper bound. The logarithmic plot reveals that both the bound separation and their uncertainty obey power laws; i.e., they converge as $CM^{-\alpha}$, where C and α are constants. Comparing the results of section III on the same plot shows that using the exact distribution to perform the MC steps lowers the prefactor, C, in the power law, but does not affect the exponent, α. The bounds converge with $\alpha \approx 1$ and the error with $\alpha \approx 1/2$. We have never observed higher respective values in any MC finite-time switching simulation, even in more complex systems, suggesting that these are limiting rate laws.

These limits can be rationalized. When the energy of a quantum state is changed by ΔE, the work done is proportional to the population of the state and to ΔE. The free energy change can be expanded as a Taylor series in ΔE, and the first term (linear in ΔE) is equal to the work. From Helmholtz's inequality, we know that the work is greater than the free energy change, and the Taylor series tells us that the first term in the discrepancy is proportional to $(\Delta E)^2$. If the overall change in the state's energy is divided into M equal steps of $\Delta E/M$, the work at each step will therefore exceed the free energy change by a term of order $(\Delta E/M)^2$. The discrepancy between the work and the free energy is in the same direction for each of the M steps, so the total difference is of order $M(\Delta E/M)^2 = (\Delta E)^2/M$; i.e., the work converges to the free energy from above as M^{-1}. This rate is borne out in practice as a limit for MC simulations, although worse convergence is certainly possible if the system is far from equilibrium at intermediate steps, as might result from a poor choice of path or reference state.

The actual work observed in a single step, where the energy level changes by $\Delta E/M$, depends on the instantaneous population of the level. Members of an ensemble exist in different states, and the work done in one step varies between members with a distribution whose width is proportional to the energy change, $\Delta E/M$. The direction of fluctuations is random, so that the distribution of the total work done in M consecutive steps is obtained by adding the contributions in quadrature. The result is an overall distribution width proportional to $M^{1/2}(\Delta E/M) = \Delta E/M^{1/2}$ to a first approximation. This width is propor-

tional to the uncertainty observed when measuring either of the upper or lower bounds in a simulation of M steps, in agreement with the limiting $M^{-1/2}$ convergence observed in Figure 8.

In contrast with the work, which reflects a change in the Hamiltonian, heat flows between the system and the heat bath even in a system at equilibrium. At equilibrium, the cumulative heat by definition has an average of zero but experiences fluctuations from a distribution of fixed width. When the external conditions are changed, for example due to work, the fluctuations in the heat persist, no matter how slowly the changes are made. This explains the relatively poor quality of the entropy bounds in Figure 2, which rely on accumulating $\delta Q/T$, compared with the free energy bounds in the other figures. Hence, finite-time variational switching is far more rewarding for the accurate calculation of free energies than of entropies.

VII. Summary

The fact that M^{-1} convergence of the free energy bounds is the fastest that can be obtained in stochastic simulations of the type investigated here, even with full knowledge of the equilibrium distribution, is an indication of how difficult it is to calculate free energies. Ultimately, the bound separation approaches the statistical error in the bounds themselves, and further precision is limited by the latter, which fall only as $M^{-1/2}$. This behavior is no worse than thermodynamic integration or free energy perturbation calculations, which are inherently statistical approaches and also converge as $M^{-1/2}$.

Despite the limiting law, sections IV and V have shown that imaginative choice of reference state and switching path can go far in reducing the prefactor of the convergence law, providing significant enhancements in overall efficiency. Certainly much is to be gained by identifying the physical bottlenecks that are specific to a given application.

The support of NSF chemistry is gratefully acknowledged. L.M.A. also acknowledges support from the NPSC and a University of Washington HPCC training grant.

References

(1) Kollman, P. Free energy calculations: Applications to chemical and biochemical phenomena. *Chem. Rev.* **1993**, *93*, 2395−2417.
(2) Alberty, R. A. Degrees of freedom in biochemical reaction systems at specified pH and pMg. *J. Phys. Chem.* **1992**, *96*, 9614−9621.
(3) Wolynes, P. G.; Onuchic, J. N.; Thirumalai, D. Navigating the folding routes. *Science* **1995**, *267*, 1619−1620.
(4) Truhlar, D. G.; Garrett, B. C.; Klippenstein, S. J. Current status of transition-state theory. *J. Phys. Chem.* **1996**, *100*, 12771−12800.
(5) Pippard, A. B. *Classical Thermodynamics*; Cambridge University Press: Cambridge, 1961.
(6) Kirkwood, J. G. Statistical mechanics of fluid mixtures. *J. Chem. Phys.* **1935**, *3*, 300−313.
(7) Zwanzig, R. W. High-temperature equation of state by a perturbation method. I. Nonpolar gases. *J. Chem. Phys.* **1954**, *22*, 1420−1426.
(8) Straatsma, T. P.; McCammon, J. A. Computational alchemy. *Annu. Rev. Phys. Chem.* **1992**, *43*, 407−435.
(9) *Finite-Time Thermodynamics and Thermoeconomics*; Sieniutycz, S.; Salamon, P., Eds.; Taylor & Francis: New York, 1990.
(10) Schön, J. C. A thermodynamic distance criterion of optimality for the calculation of free energy changes from computer simulations. *J. Chem. Phys.* **1996**, *105*, 10072−10083.
(11) Clausius, R. *The Mechanical Theory of Heat*; translated by Browne, W. R.; MacMillan: London, 1879.
(12) Metropolis, N.; Rosenbluth, A. W.; Rosenbluth, M. N.; Teller, A. H.; Teller, E. Equation of state calculations by fast computing machines. *J. Chem. Phys.* **1953**, *21*, 1087−1092.
(13) Straatsma, T. P.; Berendsen, H. J. C.; Postma, J. P. M. Free energy of hydrophobic hydration: A molecular dynamics study of noble gases in water. *J. Chem. Phys.* **1986**, *85*, 6720−6727.
(14) Reinhardt, W. P.; Hunter, J. E., III. Variational path optimization and upper and lower bounds to free energy changes via finite time minimization of external work. *J. Chem. Phys.* **1992**, *97*, 1599−1601.
(15) Hunter, J. E., III; Reinhardt, W. P.; Davis, T. F. A finite-time variational method for determining optimal paths and obtaining bounds on free energy changes from computer simulations. *J. Chem. Phys.* **1993**, *99*, 6856−6864.
(16) Schrödinger, E. *Statistical Thermodynamics*; Dover: New York, 1989.
(17) Helmholtz's contributions to various scientific disciplines are discussed in the following: *Hermann von Helmholtz and the Foundations of Nineteenth Century Science*; Cahan, D., Ed.; University of California Press: Berkeley, 1993.
(18) $V_{LJ} = 4\epsilon\sum_{i<j}[(\sigma/r_{ij})^{12} - (\sigma/r_{ij})^{6}]$, where r_{ij} is the separation of atoms i and j, and the length and energy parameters take the values $\sigma = 0.3405$ nm and $\epsilon = 119.8$ K.
(19) Amon, L. M.; Reinhardt, W. P. Development of reference states for use in absolute free energy calculations of atomic clusters with application to 55-atom Lennard-Jones clusters in the solid and liquid states. *J. Chem. Phys.* **2000**, *113*, 3573−3590.
(20) Lee, J. K.; Barker, J. A.; Abraham, F. F. Theory and Monte Carlo simulation of physical clusters in the imperfect vapor. *J. Chem. Phys.* **1973**, *58*, 3166−3180.
(21) Doye, J. P. K.; Wales, D. J. An order parameter approach to coexistence in atomic clusters. *J. Chem. Phys.* **1995**, *102*, 9673−9688.
(22) Beutler, T. C.; Mark, A. E.; van Schaik, R. C.; Gerber, P. R., van Gunsteren, W. F. Avoiding singularities and numerical instabilities in free energy calculations based on molecular simulations. *Chem. Phys. Lett.* **1994**, *222*, 529−539.
(23) Parametrization: $V(\lambda) = 4\epsilon(1-\lambda)\sum_{i<j}[(\lambda^6 + r_{ij}^6/\sigma^6)^{-2} - (\lambda^6 + r_{ij}^6/\sigma^6)^{-1}]$. The Lennard-Jones potential is recovered at $\lambda = 0$. Near $\lambda = 1$, the potential is turned off and the repulsive core is simultaneously softened.
(24) De Koning, M.; Antonelli, A.; Yip, S. Optimized free-energy evaluation using a single reversible-scaling simulation. *Phys. Rev. Lett.* **1999**, *83*, 3973−3977.
(25) Miller, M. A.; Reinhardt, W. P. Efficient free energy calculations by variationally optimized metric scaling: Concepts and applications to the volume dependence of cluster free energies and to solid−solid phase transitions. *J. Chem. Phys.* **2000**, *113*, 7035−7046.
(26) Andersen, H. C. Molecular dynamics simulations at constant pressure and/or temperature. *J. Chem. Phys.* **1980**, *72*, 2384−2393.
(27) Hoare, M. R.; Pal, P. Geometry and stability of "spherical" f.c.c. microcrystallites. *Nature Phys. Sci.* **1972**, *236*, 35−37.
(28) Khatchaturyan, A. G. *Theory of Structural Transformations in Solids*; Wiley: New York, 1983.

AR950181N